A fractal model of earthquake occurrence: Theory, simulations and comparisons with the aftershock data

Bikas K. Chakrabarti

Theoretical Condensed Matter Physics Division

Saha Institute of Nuclear Physics

Collaborators:

Pathikrit Bhattacharyya (Princeton Univ., Princeton)
Pratip Bhattacharya (Gurudas Coll., Kolkata)
Kamal (IIT, Roorkee)
Srutarshi Pradhan (SINTEF, Trondheim)
Robin Stinchcombe (Oxford Univ., Oxford)

Publications:

Rev. Nonlin. Sc. & Complexity (Wiley, 2009)
J. Phys. Conf. Series **319** (2011)

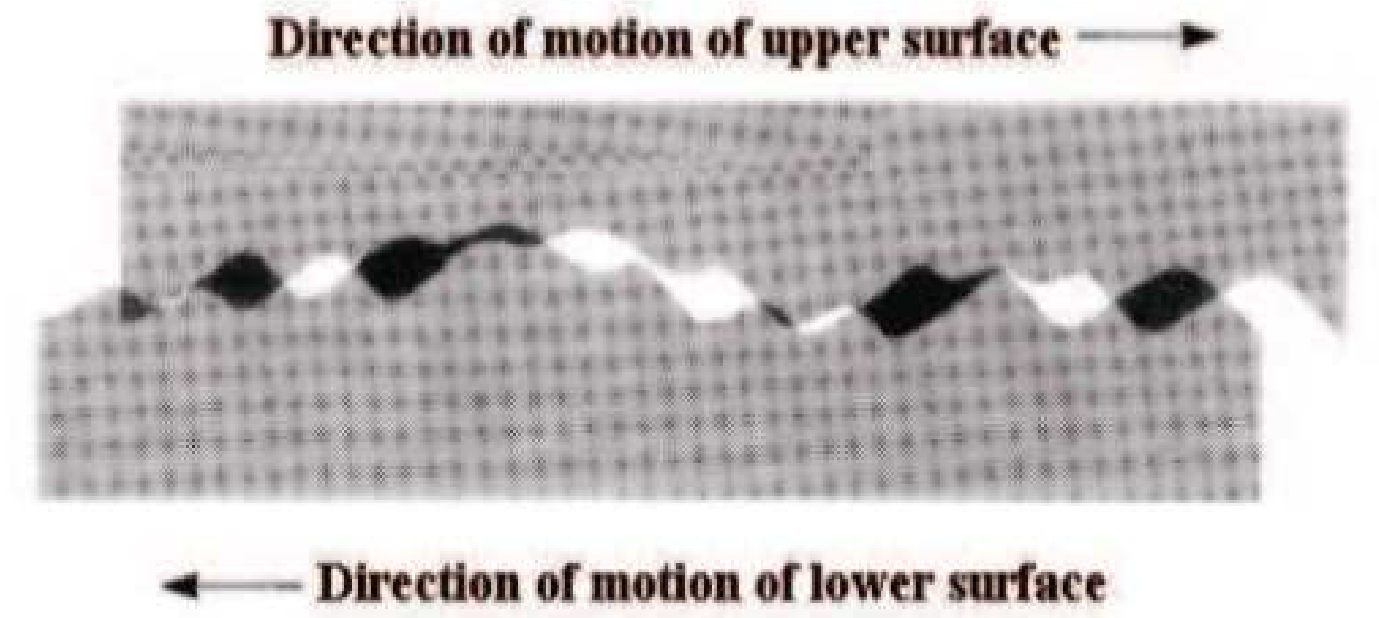

A cartoon showing overlap of two fractal surfaces. The sticking is due to interlocking of the asperities. Stress energy is accumulated and released at every slip.

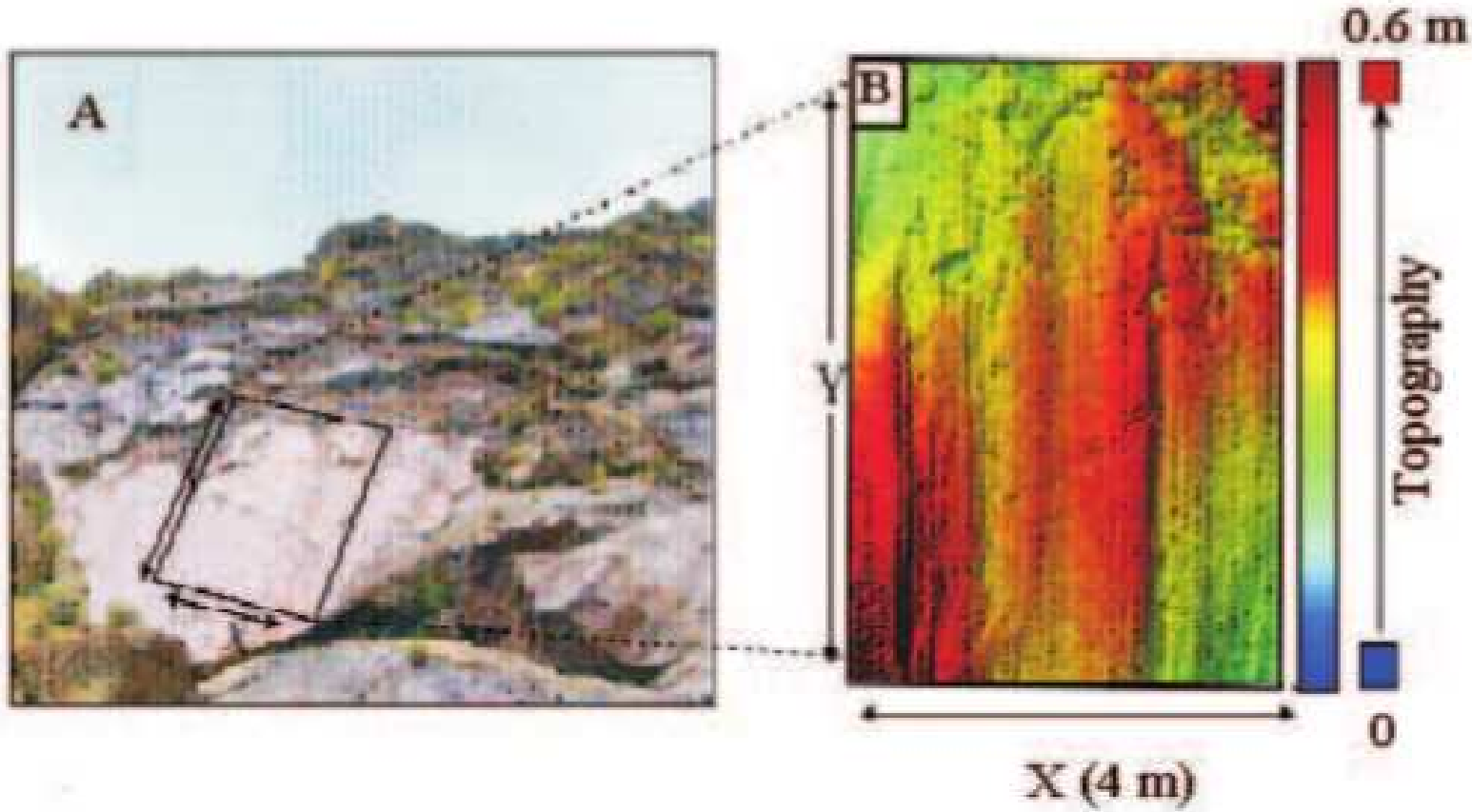

A) Chapter of a partly eroded slip surface at the Mirrors locality on the Dixie Valley fault. B) LiDAR fault surface topography as a color-scale map rotated so that the X-Y plane is the best-fit plane to the surface.

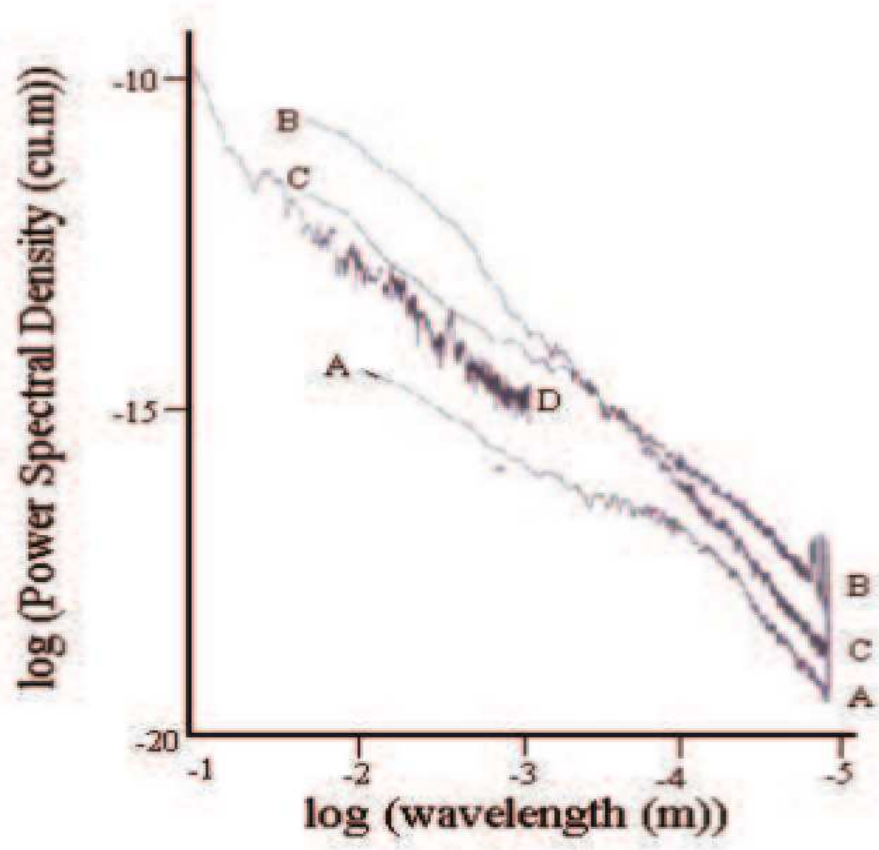

Power spectra for the fault surfaces studied in the Dixie Valley. A, B, C are from 10 – 20 mm long lab profiles. D is part of a spectrum from a 1 m long field profile. A – smoothest, unweathered hand sample of surface. B – sugary weathered surface. C – surface that apparently a is composite of sub-parallel surfaces.

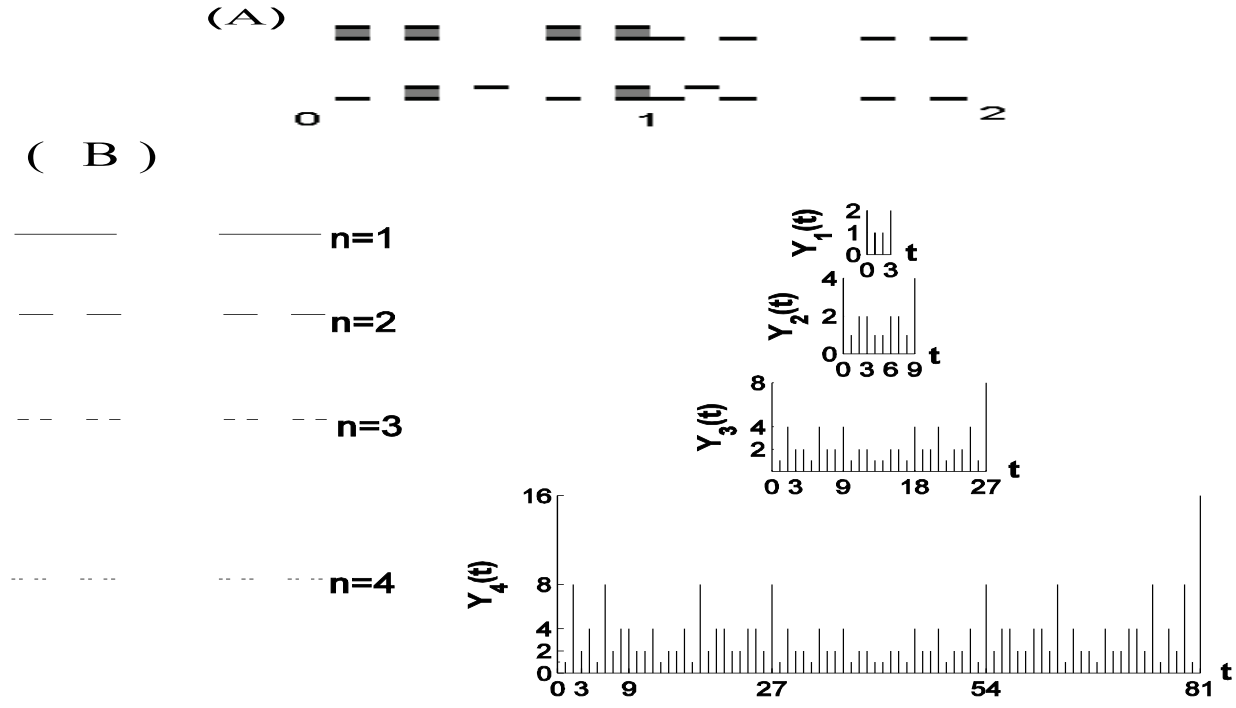

(A) The recursive structure of the time series for the first four generations in the fractal-fractal overlap model. On the left the respective Cantor set generations are shown. Noticeable is the fact that the time series of all preceding generations are embedded within the time series at a given generation.

(B) A realization of the model for the second generation at t=0 and at t=2. The overlapping segments are shaded in grey. The lower Cantor set is repeated between 1 and 2 to employ the periodic boundary condition. The upper Cantor set slides over the lower.

$$Pr(2^{n-k}) = \left(\begin{array}{c} n \\ n-k \end{array} \right) \left(\frac{1}{3}\right)^{n-k} \left(\frac{2}{3}\right)^{k}$$

$$Y_n = 2^{n-1} \& m = \ln_2 Y_n \Rightarrow Pr(m) = \left(\begin{array}{c} n \\ m \end{array} \right) \left(\frac{1}{3}\right)^{m} \left(\frac{2}{3}\right)^{n-m}.$$

$$F(m) = \frac{3}{2\sqrt{n\pi}} \exp\left(-\frac{9}{4}\frac{(m-n/3)^2}{n}\right),$$

$$F_{cum}(m) = \int_m^\infty F(m')dm' = \int_m^\infty \frac{3}{2\sqrt{n\pi}} \exp\left(-\frac{9}{4}\frac{(m'-n/3)^2}{n}\right) dm'.$$

$$F_{cum}(m) = \frac{3}{4\sqrt{n}} \mathrm{erfc}\left(\frac{3(m-n/3)}{2\sqrt{n}}\right).$$

$$F_{cum}(m) = \frac{1}{2\sqrt{\pi}} \exp\left(-n/4\right) \exp\left(\frac{-9m^2}{4n} + \frac{3m}{2}\right) (m-n/3)^{-1}.$$

$$\log N(m) = A - \frac{3}{4}m - \log(m - n/3), \qquad \boxed{\text{GR Law}}$$

$$N(t) = \log_3 t \Rightarrow \frac{dN}{dt} = t^{-\rho}, \rho = 1 \qquad \boxed{\text{Omori Law}}$$

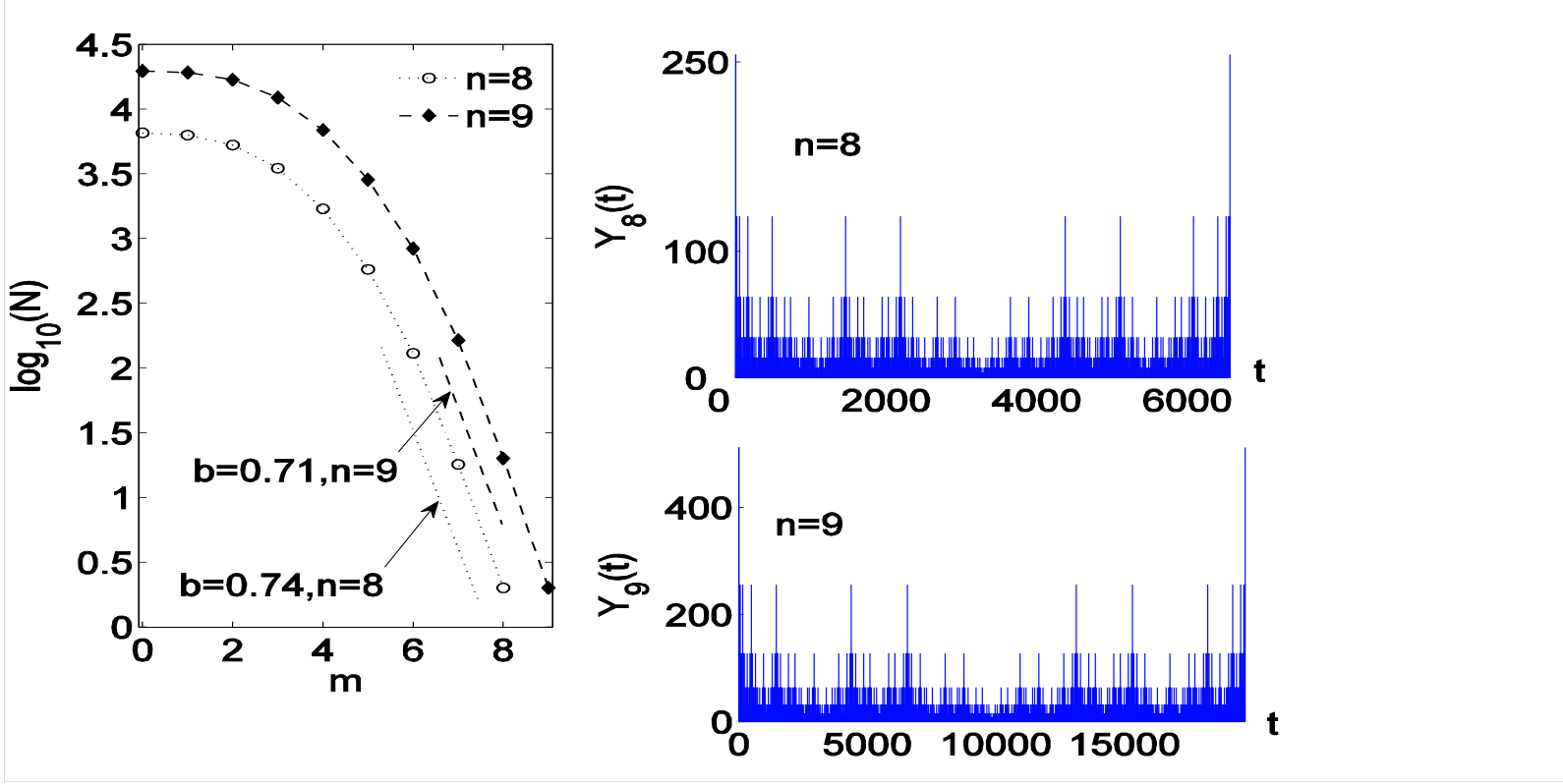

The Frequency-Magnitude (FM) plots ($\log N(m)$ vs. magnitude m, N being the number of earthquakes with magnitude greater than or equal to magnitude m) for the model for generations 8 and 9. The overlap time series are also shown on the right for the respective generations. The low-magnitude roll-off is evident for both the generations. The lines are drawn as visual aid to understand the linear trend. The b-values were obtained by fitting a linear polynomial to the data. The values of the exponents are the slopes of the indicated straight lines. The b-values thus obtained are also indicated for each of the generations.

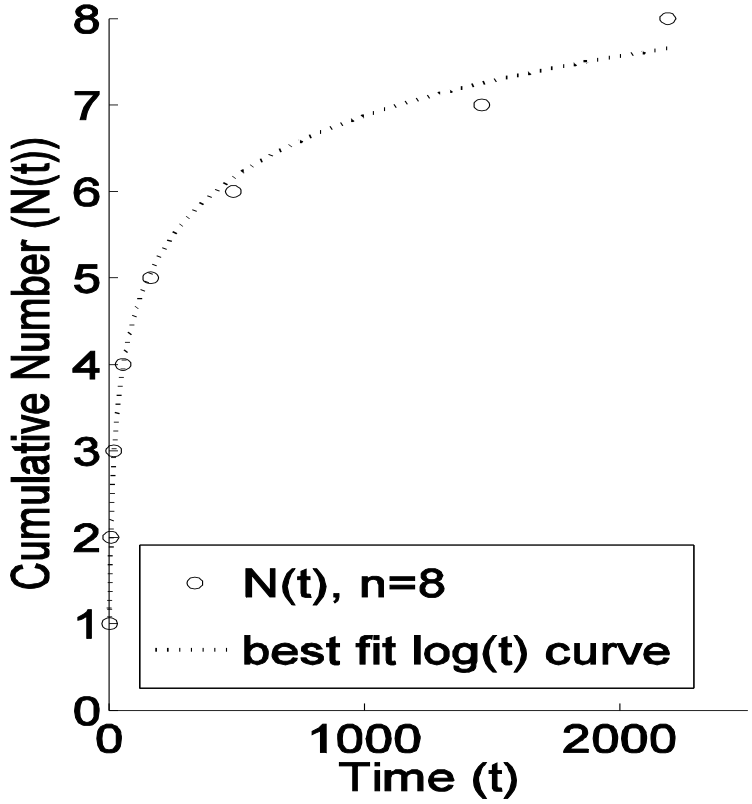

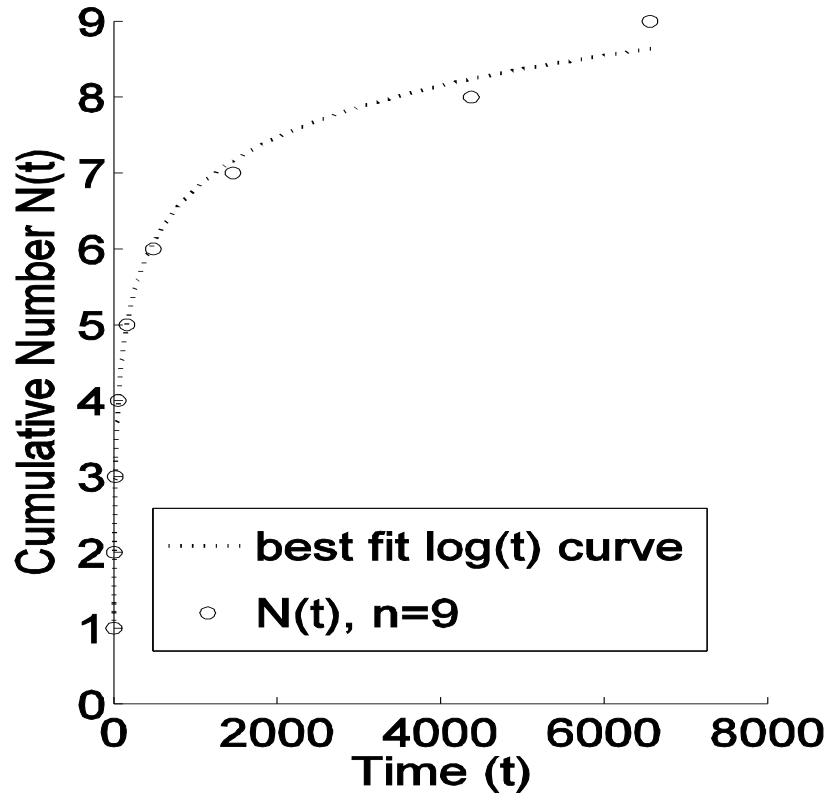

Omori Law from the model for generations 8 and 9 respectively. Dashed lines show best logarithmic fits. Plots are for $N(t)$ vs. t, $N(t)$ being cumulative number of aftershocks at time t where t is the time since the mainshock. Time parameter for the model being as defined in the text i.e. unit time for a step of size 3^{-n}.

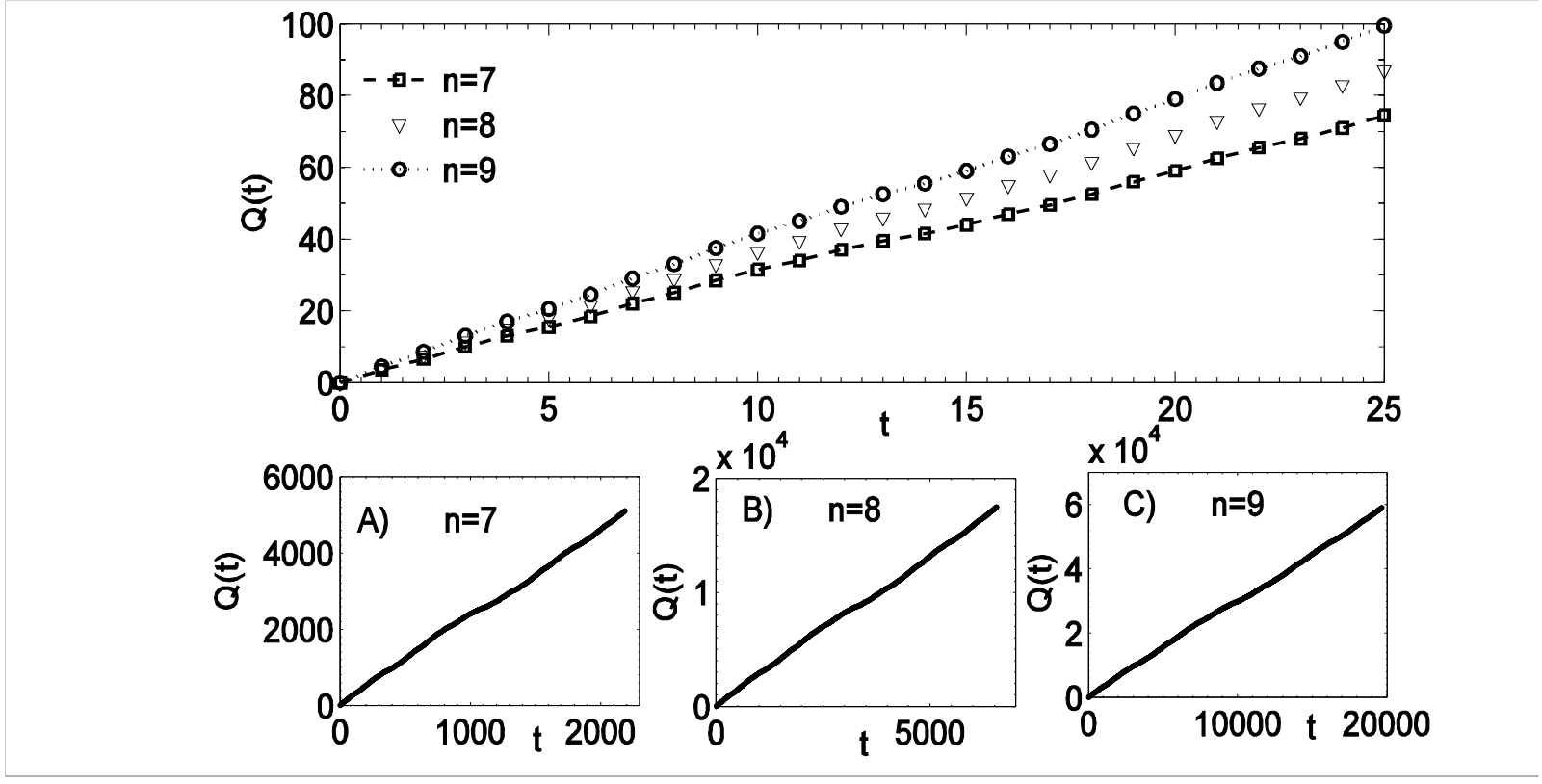

The $Q(t)$ vs. t statistic for the model for generations 7, 8 and 9. At the top plots for all the three generations (for the first 25 time steps) are shown together to show the increase in slope with increase in generation number n. At the bottom plots A), B) and C) show the entire $Q(t)$ time series for generations 7, 8 and 9 respectively.

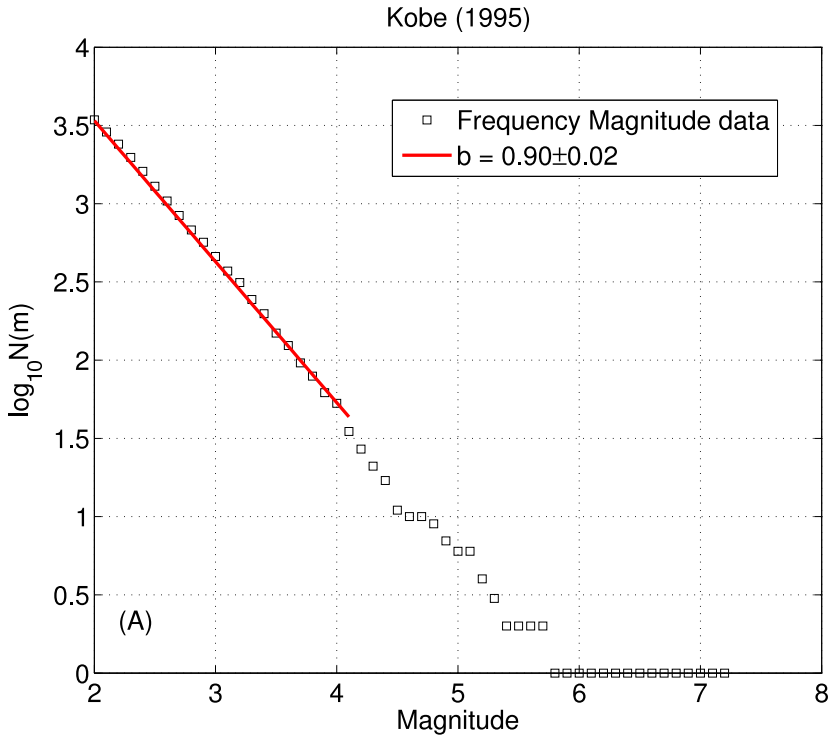

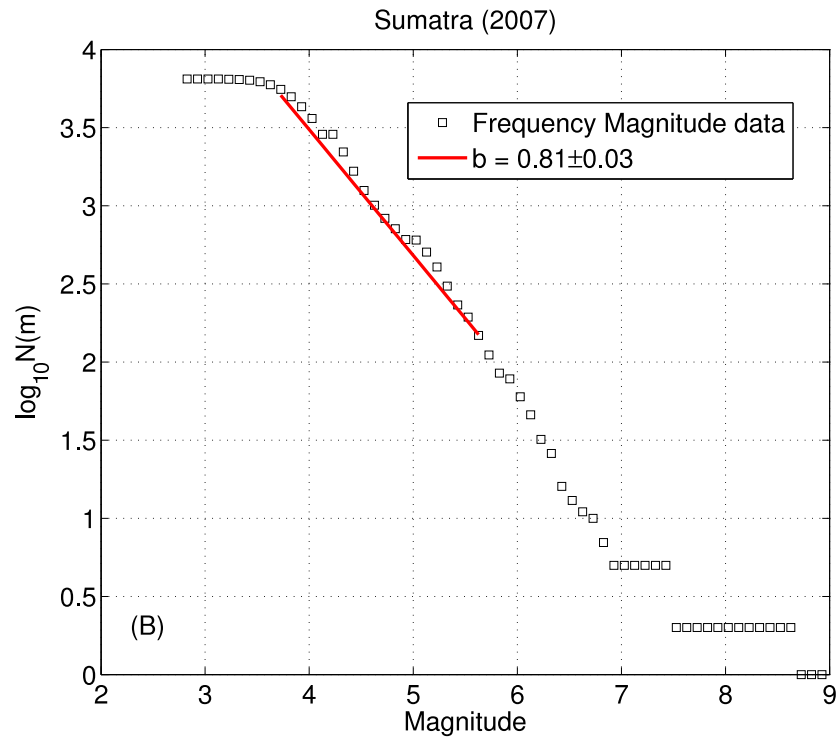

GR or Frequency-Magnitude distributions for the aftershock sequences described in the text A) the 1995 Kobe earthquake and B) the 2004 Sumatra earthquake. We clearly see the lower magnitude roll-off from the power law distribution in Sumatra. $N(m)$ represents number of earthquakes with magnitude greater than or equal to m, m represents magnitude.

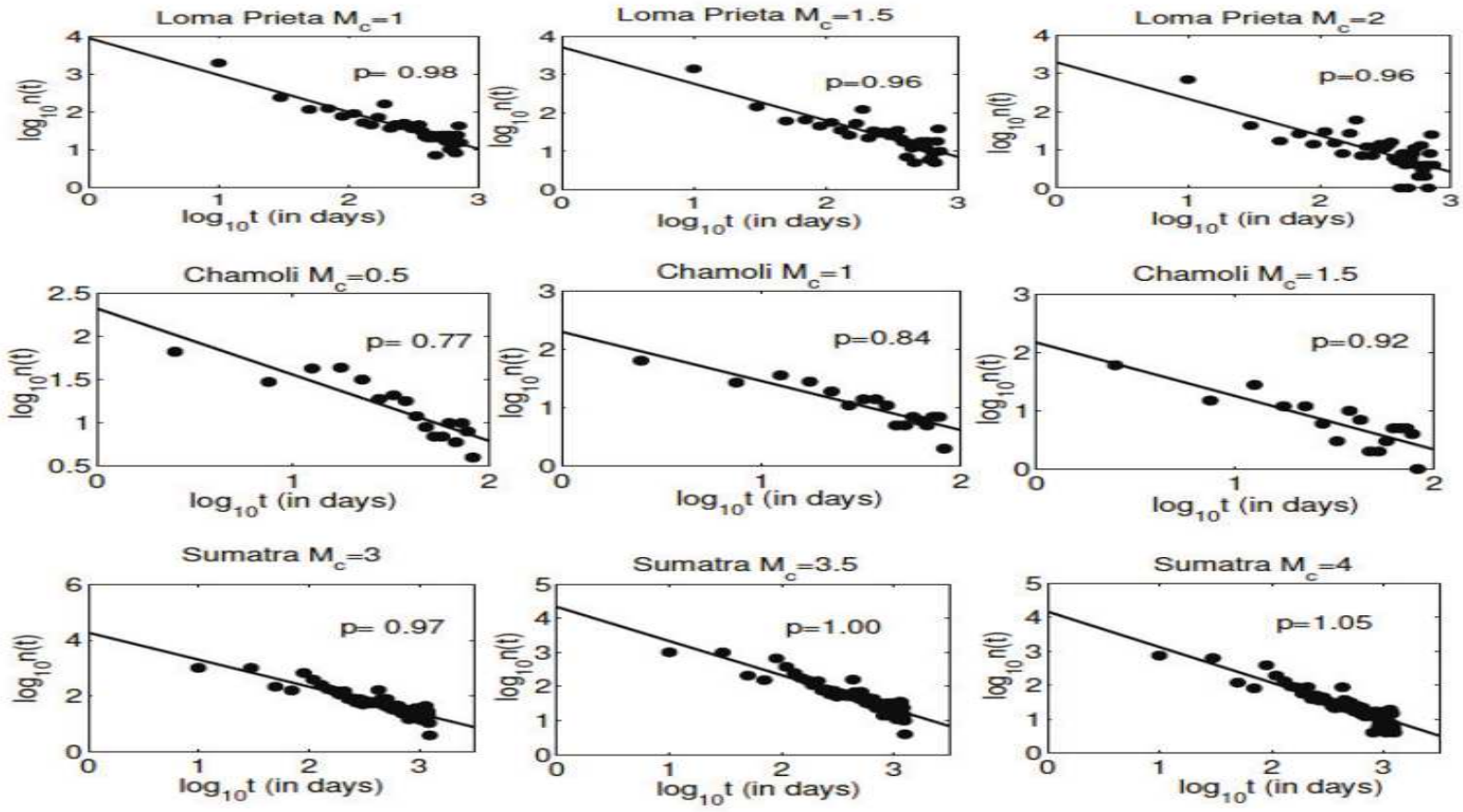

The plots for number of aftershocks per unit time $n(t)$ vs. time since the mainshock in days, t, for the Loma Prieta, Chamoli and Sumatra data sets. The cut-off magnitudes M_c are indicated in each plot title. The corresponding p values are shown within the plots. The solid lines give the linear fits to the data with slope p.

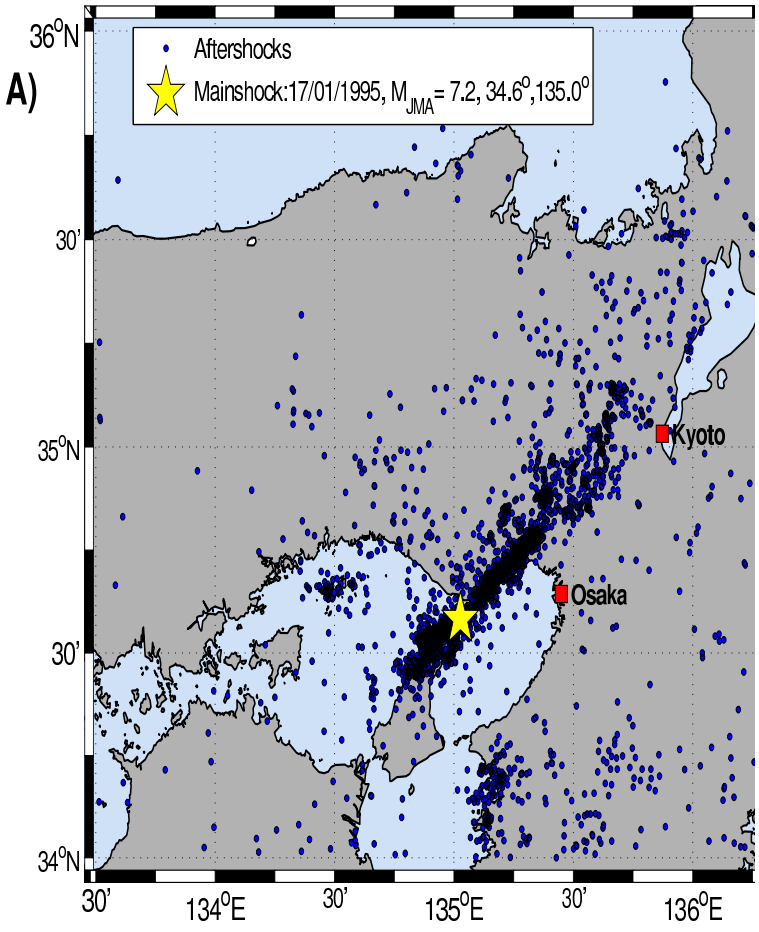

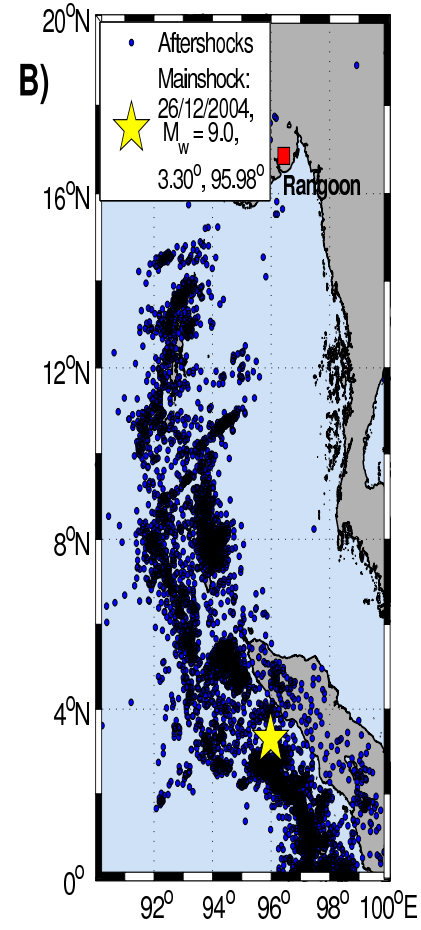

Maps showing spatial distribution of aftershocks chosen for A) Kobe, B) Sumatra datasets.

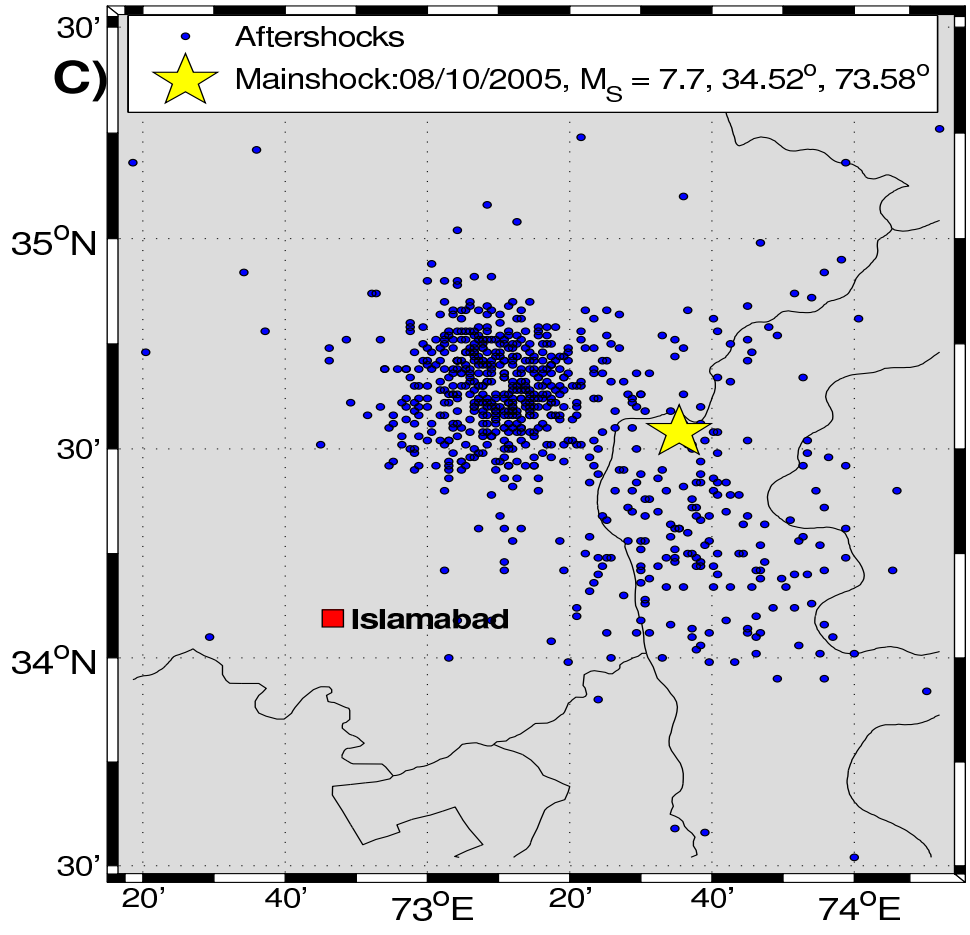

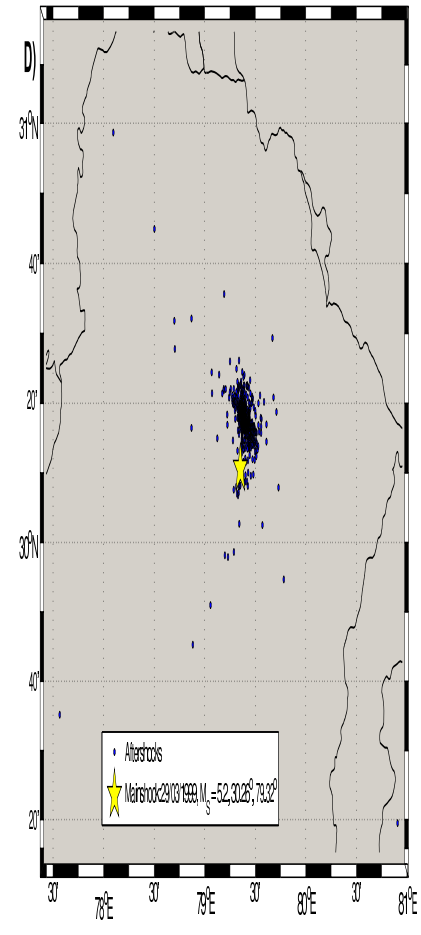

Maps showing spatial distribution of aftershocks chosen for A) Muzaffarabad, B) Chamoli datasets.

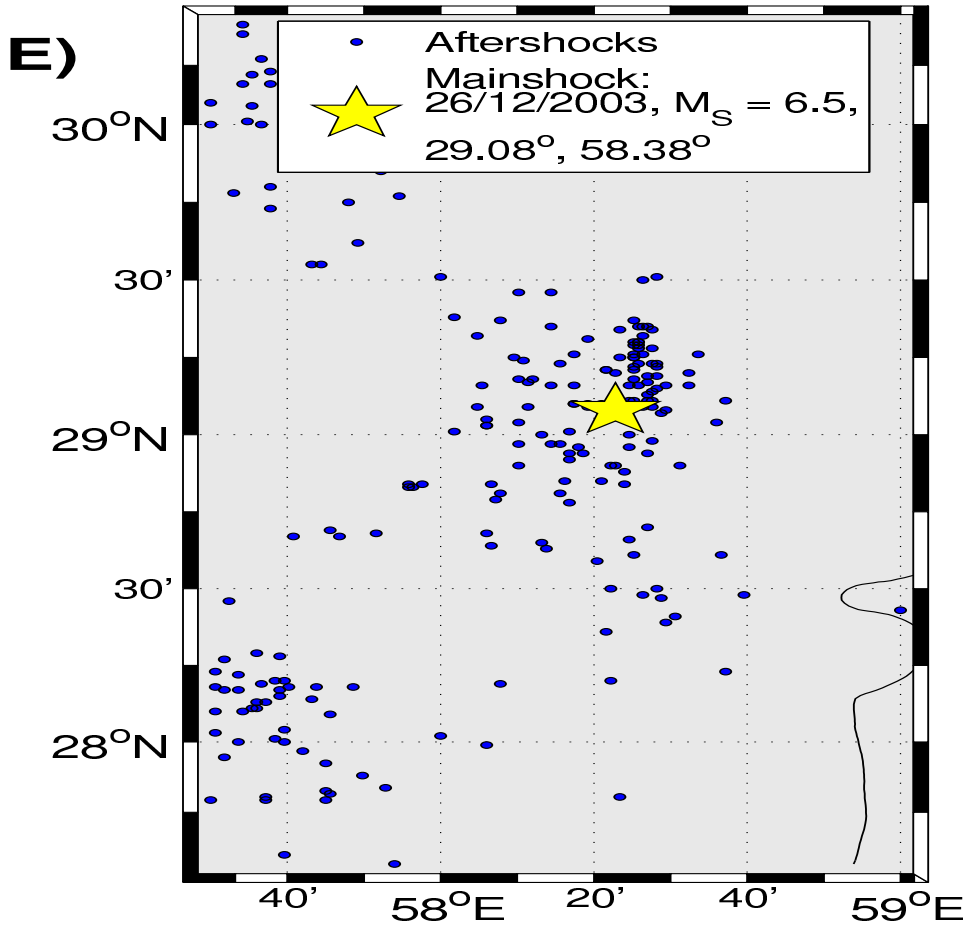

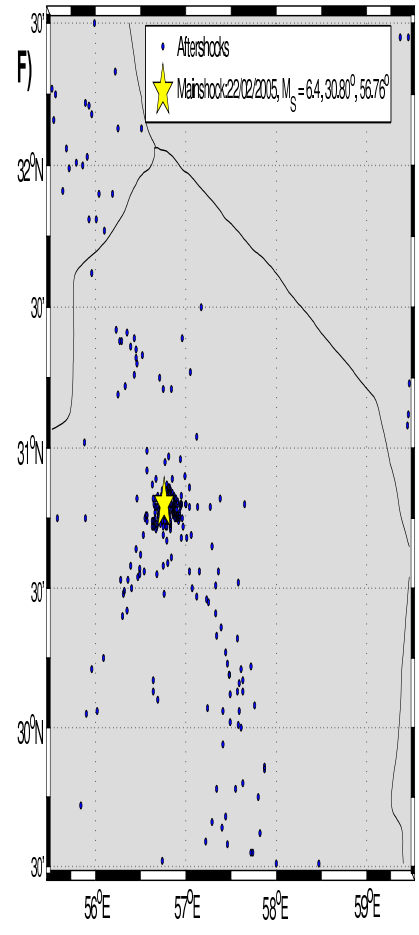

Maps showing spatial distribution of aftershocks chosen for A) Bam, B) Zarand datasets.

G)

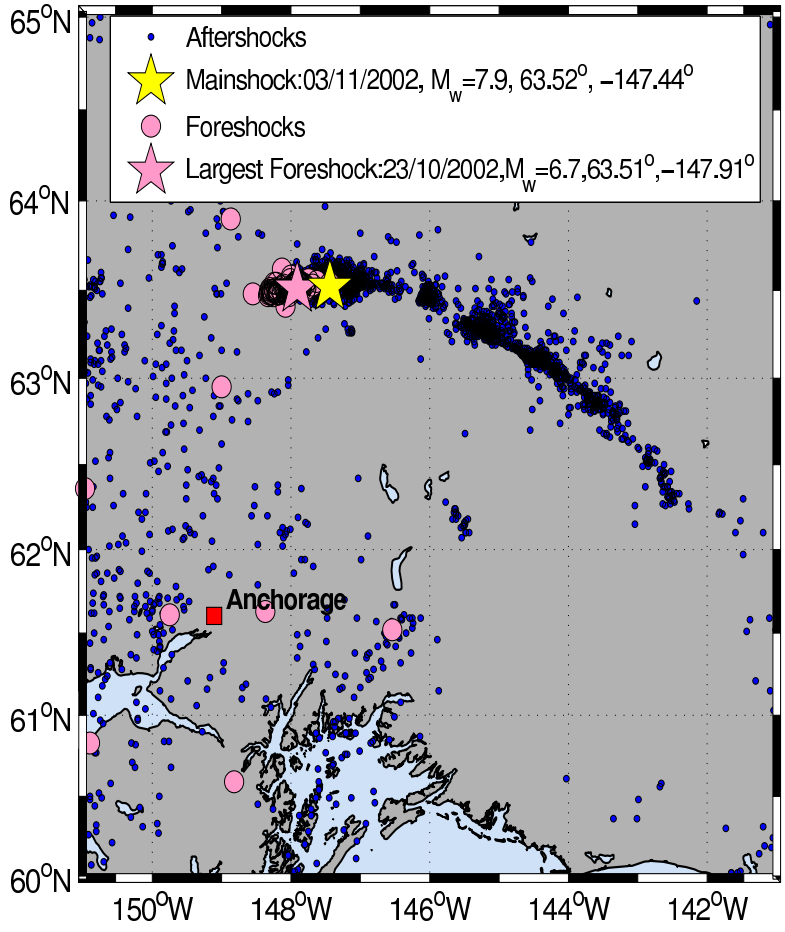

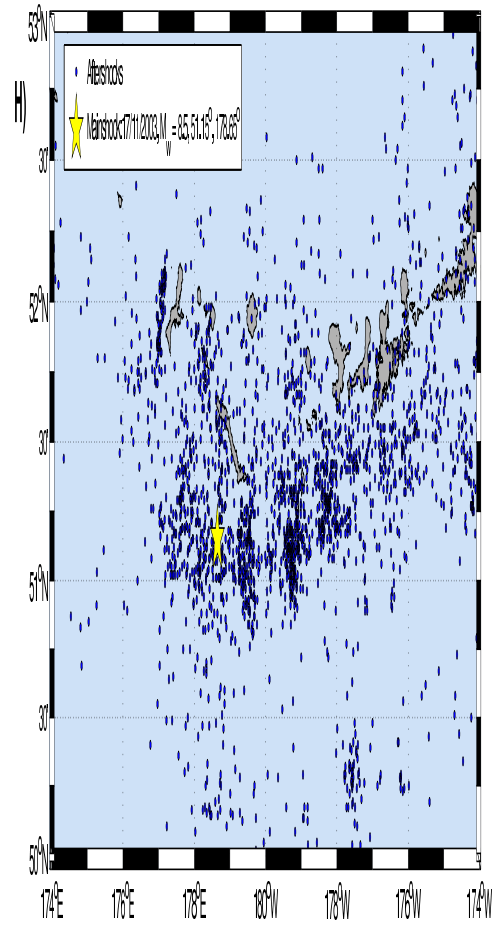

Maps showing spatial distribution of aftershocks chosen for A) Alaska1, B) Alaska2 datasets.

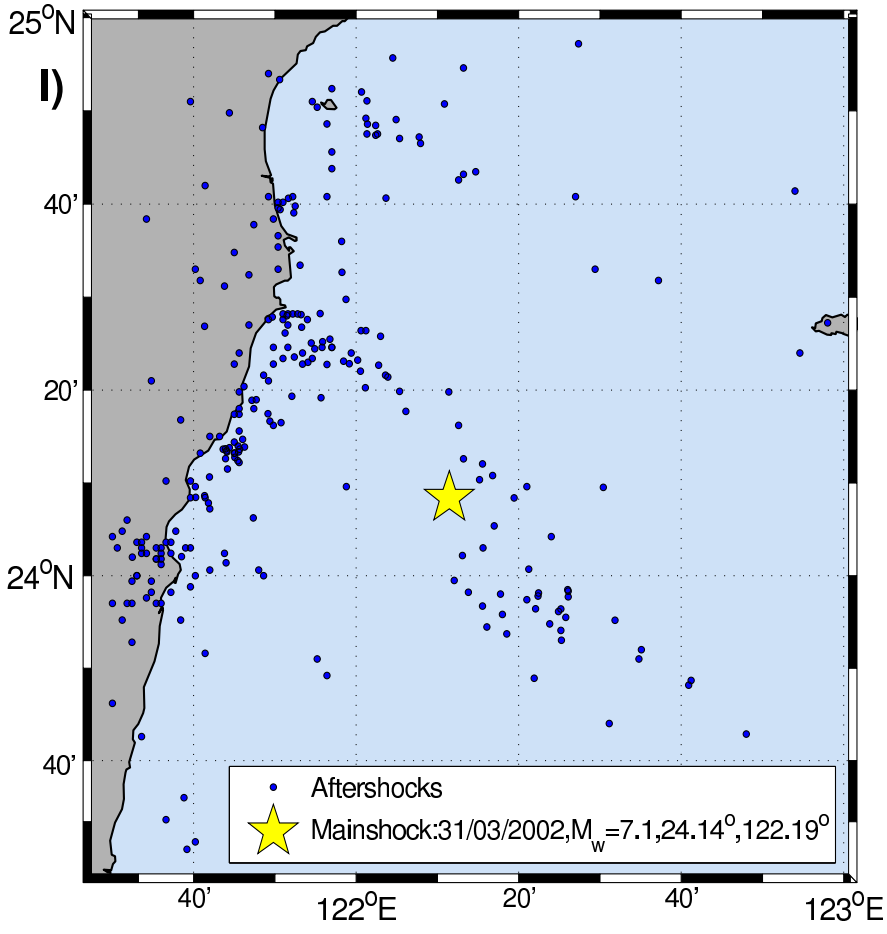

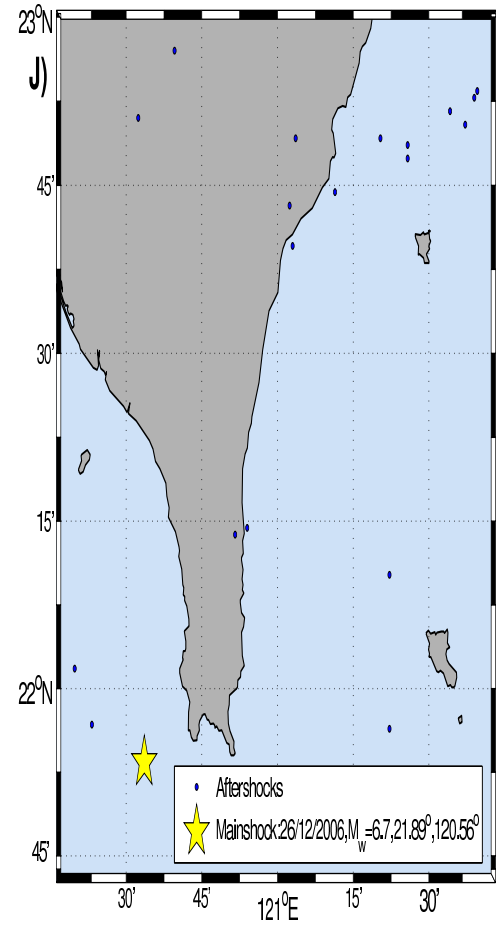

Maps showing spatial distribution of aftershocks chosen for A) Taiwan1, B) Taiwan2 datasets.

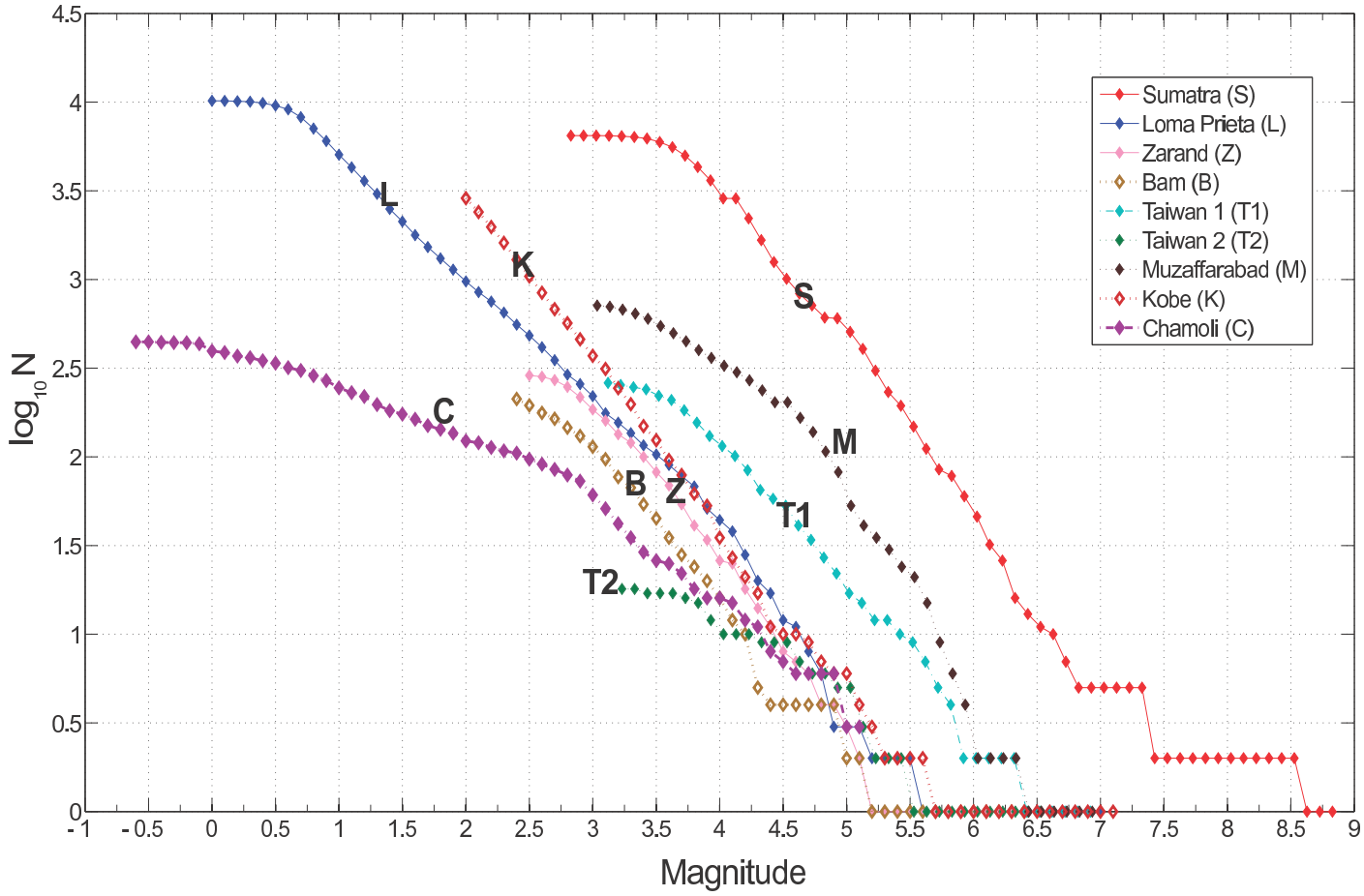

The Frequency-Magnitude distributions for the various aftershock sequences (except for the Alaska 1 and Alaska 2 sequences).

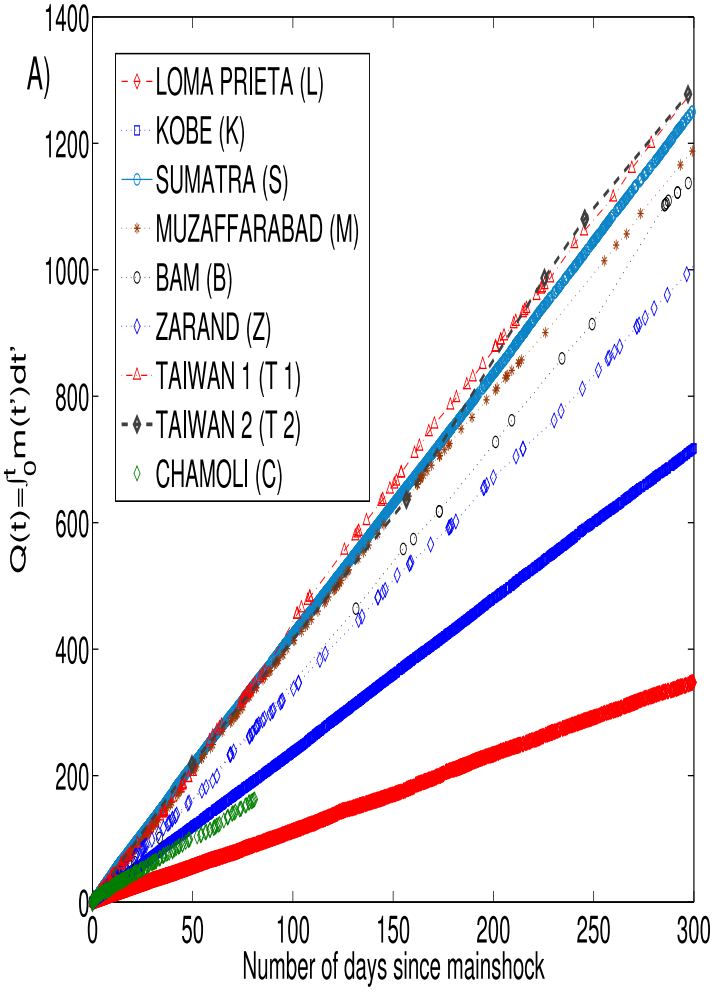

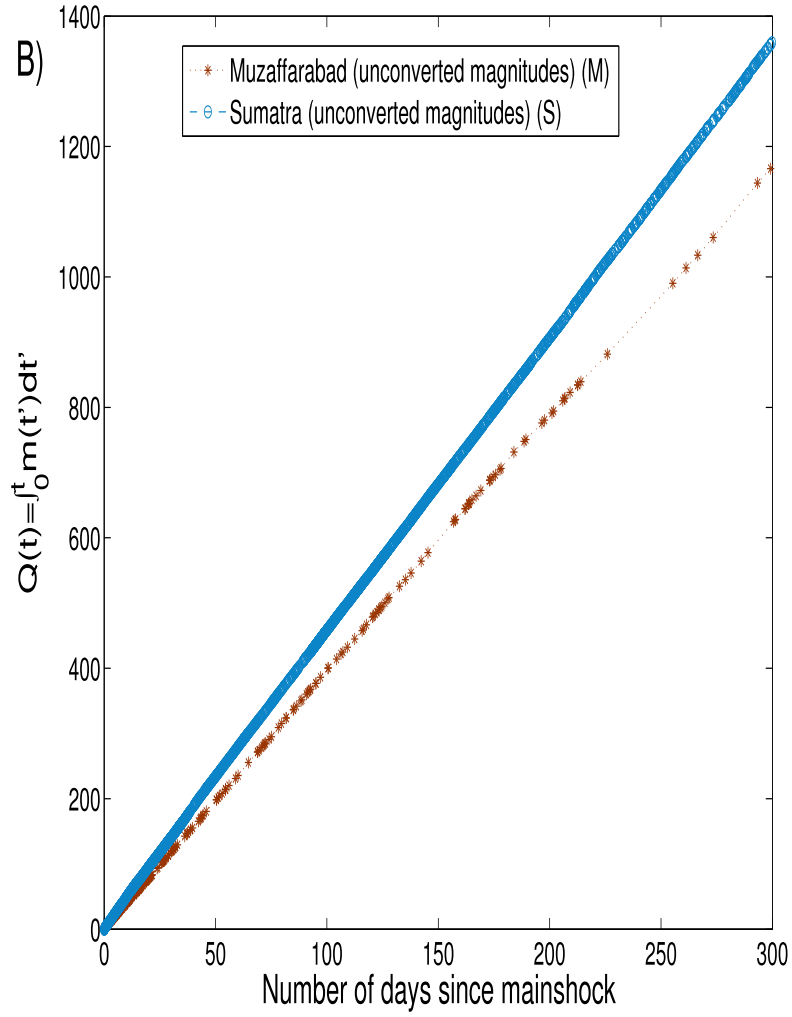

(A) Plots of time cumulant of magnitude $Q(t)$ vs. t (in number of days since the mainshock) for the first 300 days.

(B) Plots of $Q(t)$ vs. t for the Sumatra and Muzaffarabad sequences before conversion of magnitudes for the first 300 days.

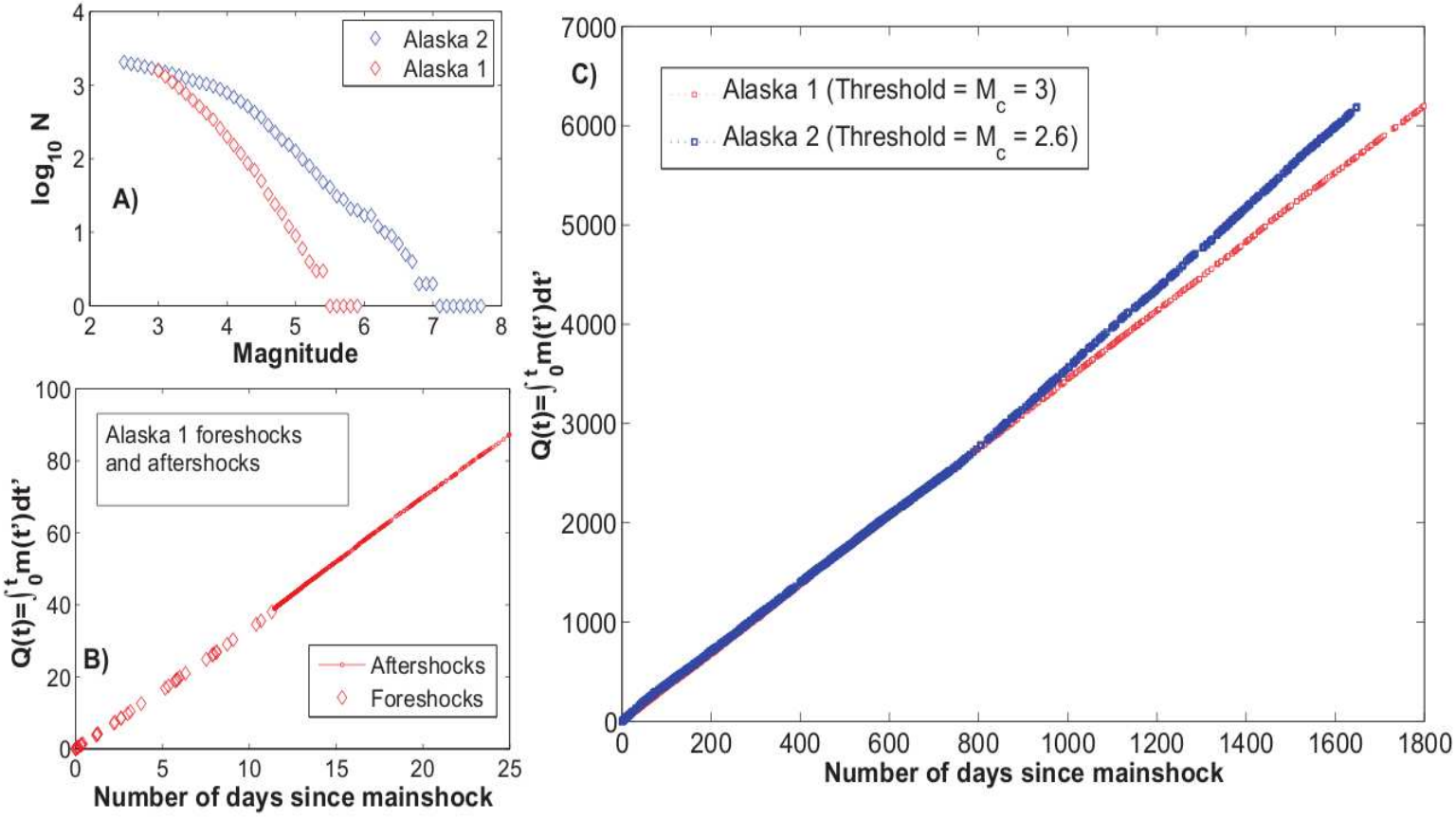

A) The frequency magnitude distribution (FMD) plots for Alaska 1 and Alaska 2. As noted in the text, the FMD for Alaska 1 is computed on the $\mathrm{M_L}$ listing. For Alaska 2 the FMD was calculated on the entire inhomogeneous listing.

B) $Q(t)$ for the first 25 days for Alaska 1 showing that foreshocks and aftershocks exhibit same slope. C) The entire sequences for Alaska 1 and 2. Note slope change in Alaska 2.

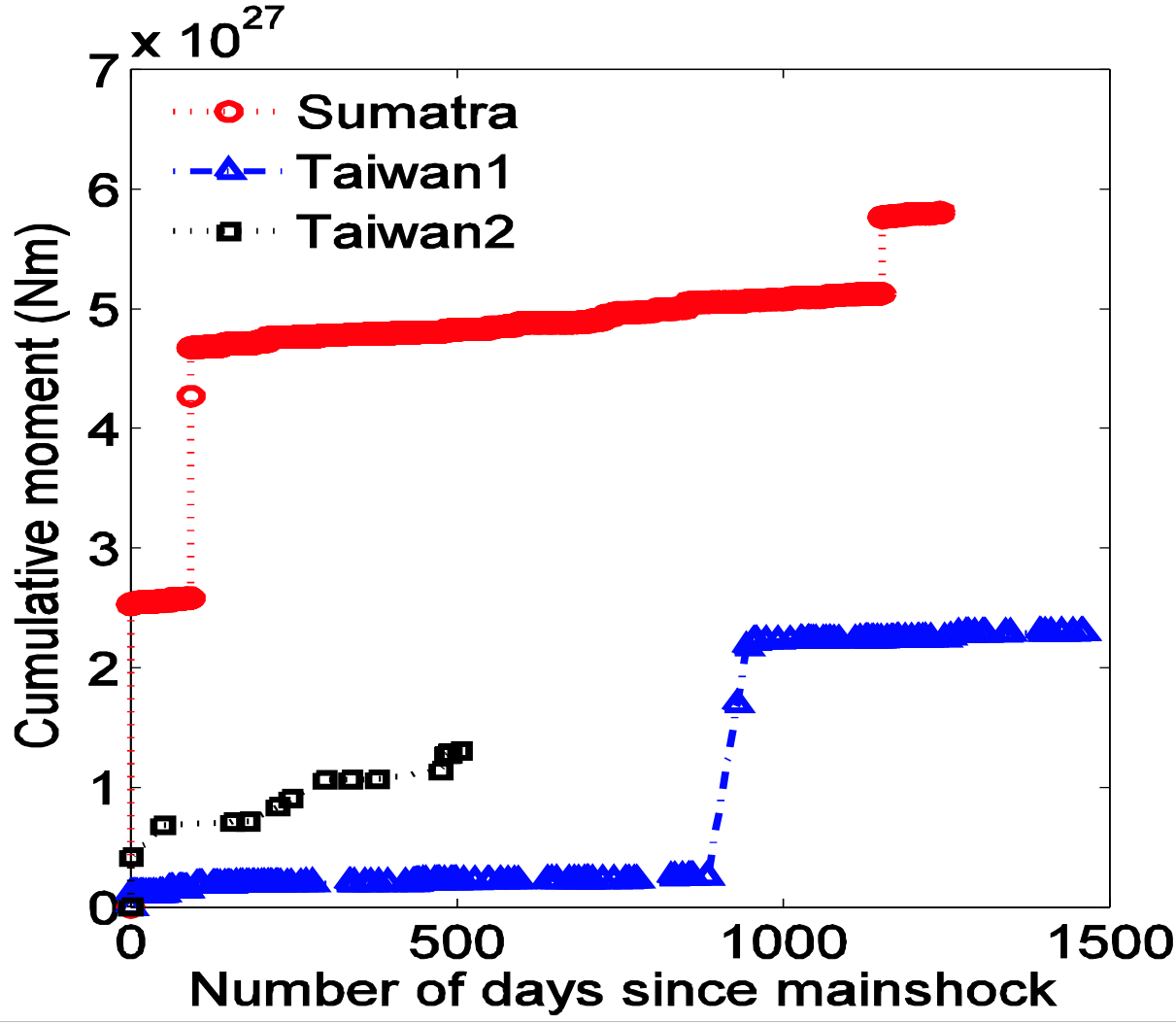

Plots of cumulative moment versus time since the mainshock for the datasets Sumatra, Taiwan 1 and Taiwan 2. The values for Taiwan 2 depicted here in the plot are 10 times the real values to ensure proper legibility of the figure.

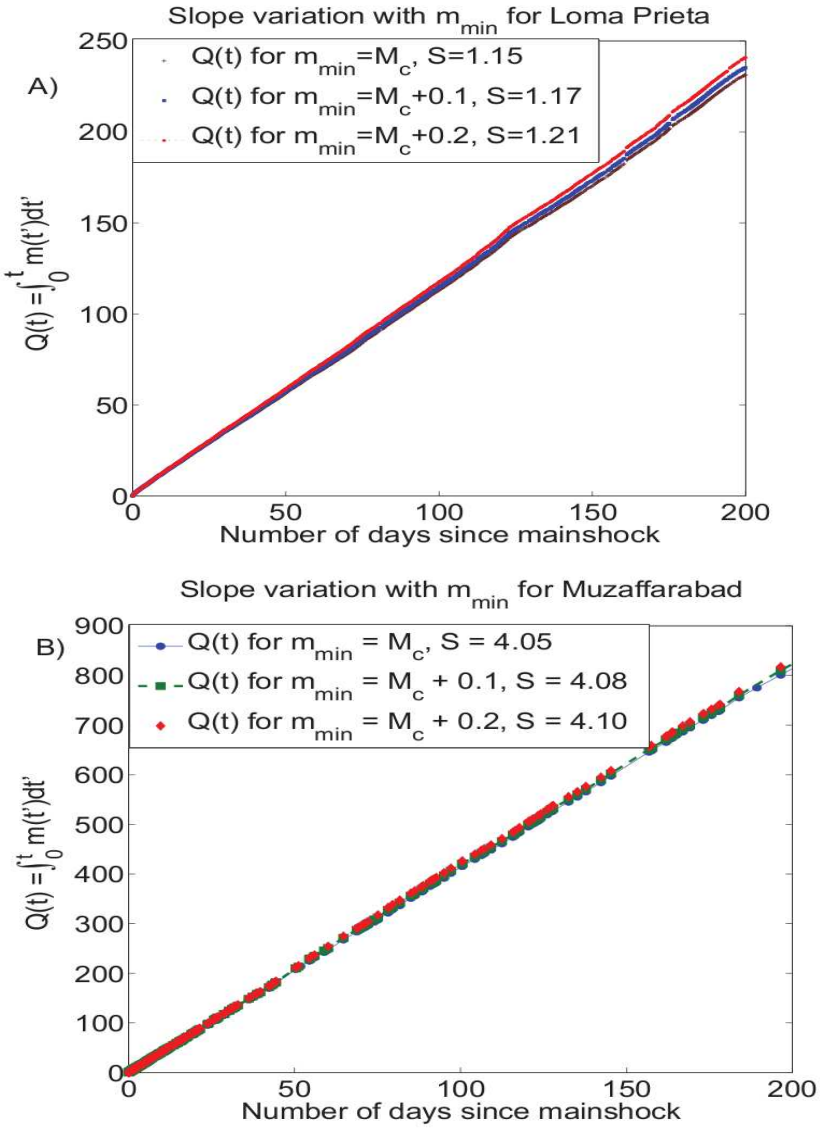

Slope variation in $Q(t)$ with $m_{\min}$ for the aftershock sequences in LomaPrieta and Muzaffarabad. First 200 days shown for the sake of clarity.

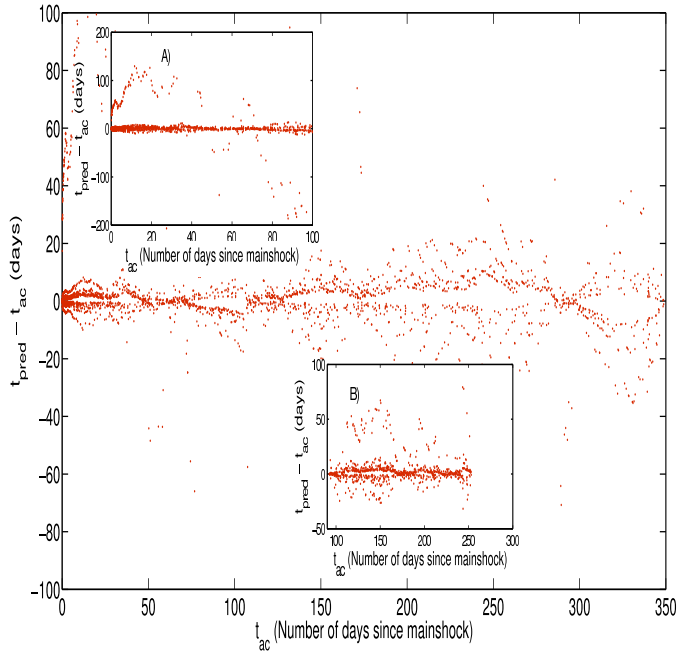

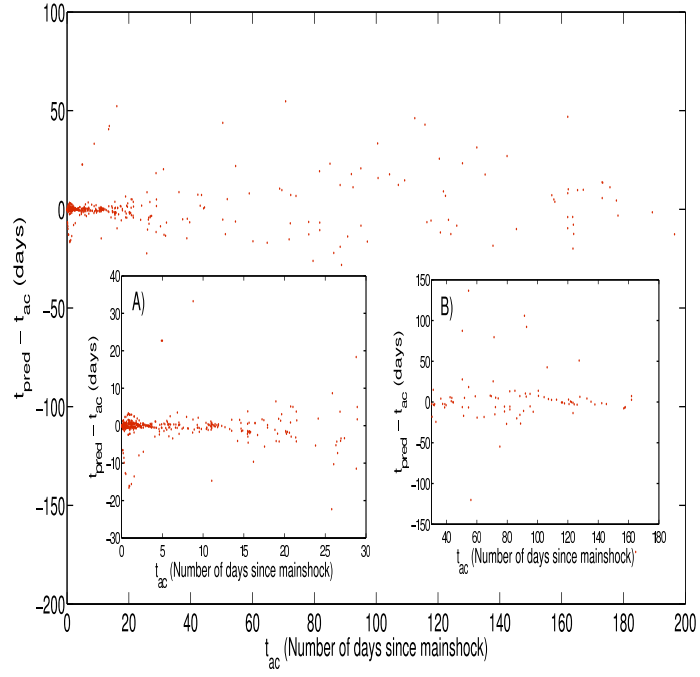

The $t_{\rm pred} - t_{\rm ac}$ vs. $t_{\rm ac}$ plots for the Kobe (top) and Muzaffarabad (bottom) sequences for first 350 and 200 days respectively. Some of the larger deviations from $y = t_{\rm pred} - t_{\rm ac} = 0$ lie beyond the extent of the y-axis shown here and are omitted to facilitate better viewing. Inset: different time windows within which $Q(t)$ was recalculated. For Kobe: Inset A) First 100 days only. Inset B) Between 90 and 250 days. Scatter lessened significantly with respect to the same time window when we integrate $Q(t)$ from the aftershock at the time origin of the window rather than the mainshock. For Muzaffarabad: Inset A) First 30 days. Inset B) Between 30 to 160 days. Again note the reduced scatter with respect to the same time window when we integrate $Q(t)$ from the aftershock at the time origin of the window rather than the mainshock.

THANK YOU